The role of gold nano-clusters supported on TiO_2(110) model catalyst in CO oxidation reaction

Anton Visikovskiy[1], Kei Mitsuhara[2], and Yoshiaki Kido[2]

[1] *Department of Appl. Quantum Phys. & Nucl. Eng., Kyushu University, Fukuoka, 819-0395, Japan*

[2] *Department of Physics, Ritsumeikan University, Kusatsu, Shiga-ken 525-8577, Japan*

Abstract

It was reported previously that O adatoms adsorbed dissociatively on the 5-fold Ti rows of rutile TiO_2(110) made the surface O-rich and reacted with CO molecules to form CO_2. An electronic charge transfer taking place from gold nano-clusters to the O-rich TiO_2(110) support played a crucial role to enhance the catalytic activity[J. Chem. Phys. **136**, 124303 (2012)]. In this study, we have further accumulated experimental data for the CO oxidation reaction enhanced by gold nano-clusters on the TiO_2(110) surface. Based on the results obtained here and previously, we propose an "interface dipole model", which explains the strong activity of Au nano-clusters supported on O-rich TiO_2(110) in CO oxidation reaction. Simultaneously, we also discuss the cationic cluster model proposed by Wang and Hammer[Phys. Rev. Lett. **97**, 136107 (2006)] and the d-band model predicted by Hammer and Nørskov[Adv. Catal. **45**, 71 (2000)]. The latter is, in particular, widely accepted to explain the activities of heterogeneous catalysts. Contrary to the d-band model, our *ab initio* calculations demonstrate that the d-band center for Au nano-clusters moves apart from the Fermi level with decreasing the cluster size and this is due to contraction of the Au-Au bond length.

I. INTRODUCTION

Since Haruta[1] discovered the catalytic activity of gold nano-clusters with a size below 5 nm, the mechanism of the emerging activity in CO oxidation reaction has been investigated from both experimental and theoretical view points. The catalytic activities reported so far were dependent on support materials and strongly enhanced with decreasing the cluster size[2-8]. In spite of many efforts, there are still many unknown and uncontrollable factors in the real catalysts. Therefore, it is a short cut to employ model catalysts for clarifying the mechanism. There are mainly three representative models that explain the emerging catalytic activity of Au nano-clusters. The first one is a geometric model stating that the fraction of active under-coordinated atoms located at corners and edges increases with decreasing the cluster size[9]. In particular, the fraction of corner atoms in the top half of a truncated octahedron clusters increases significantly for the size less than 4 nm and scales approximately as d^{-3} as the diameter (d) of the cluster shrinks[10]. The second model is based on quantum size effects upon the electronic structure of clusters[5,11]. The most widely accepted one is the d-band model, which claims that catalytic activities are enhanced as the d-band center position (E_d) moves to the Fermi-level (E_F) of a transition metal (catalyst). This is explained as follows; for dissociative adsorption of molecules on the metal surface. Hybridization of the wave functions of an adsorbate molecule and the d-state of the metal creates bonding and anti-bonding states and a potential barrier is formed for the occupancy of the anti-bonding state owing to the repulsive nature of the wave functions[12]. Hammer and Nørskov[12-14] proposed the "*d-band model"* based on this idea, which asserted that the closer the d-band center position (E_d) to the Fermi level (E_F), the smaller the occupation number of the anti-bonding state, and thereby leading to a lower potential barrier for the dissociative adsorption, It is predicted that the E_d value shifts toward the E_F with decreasing the average coordination number, particularly, with decreasing the size of metal clusters. The third one is the "cationic cluster model" proposed by Wang and Hammer[15], who showed by employing the density functional theory (DFT) that an electronic charge transfer takes place from Au clusters to an O-rich TiO_2(110) surface denoted by *O*-TiO_2(110) with O adatoms (O_{ad}) adsorbed on the 5-fold Ti rows and thus Au atoms at the interface become cationic, allowing for binding O_2 with a large adhesion energy. This means that reducible oxides are more capable of forming O-rich gold/support interfaces leading to a strong catalytic activity[16]. Hereafter, this is assigned by "*cationic cluster model*". Via many experimental and theoretical investigations, we have recently arrived at a consensus that the perimeter interface of Au/TiO_2 is the reaction site for CO oxidation[15,17-21].

In the previous study using the Au/rutile-TiO_2(110) model catalyst, we found that the O_{ad} atoms adsorbed on the 5-fold Ti rows reacted with CO to form CO_2 at room temperature (RT) and the number of the O_{ad} atoms reacting with CO was enhanced strongly by the presence of Au nano-clusters[21,22]. Importantly, an electronic charge transfer occurred from Au nano-clusters to *O*-TiO_2(110) supports, which was clearly observed quantitatively by work function measurements using synchrotron-radiation-light induced secondary electron emission. In contrast, deposition of Au nano-clusters on reduced-TiO_2(110) surfaces resulted in a reverse electronic charge transfer from the TiO_2 support to Au clusters. This result is quite consistent with the DFT calculations[15,23].

In the present work, we have confirmed the fact that the presence of Au nano-clusters enhances the number of O_{ad} atoms by measuring the gap state intensity and work function. In addition, Au nano-clusters also enhance the CO oxidation reaction. The above facts are explained by an "*interface dipole model*", which will be discussed later in comparison with the *cationic cluster model*[15]. We also measured the d-band center position with respect to the Fermi level as a function of Au-cluster size and found out the fact that the d-band center as well as d-band width and apparent $d_{3/2,5/2}$ spin-orbit splitting changed rapidly below a critical cluster size about 150 Au atoms per cluster but the d-band center position moved apart from the Fermi level[24]. This fact is controversial with the *d-band model*[14,25]. In this study, we clarify the reason why the observed d-band center shifts apart from the Fermi level with decreasing the Au cluster size based on the DFT calculations using the Vienna *ab initio* simulation package (VASP)[16,27].

II. EXPERIMENTAL

Gas phase redox reactions on oxide surfaces progress via transfer of an electronic excess charge. In the case of rutile TiO_2(110), the electronic excess charge appears in the band gap, which was identified as a Ti 3d electron bound by a positive core of Ti^{4+} ion, namely existing as a Ti^{3+} ion[28,29]. The gap state originates from (i) bridging O (O_{br}) vacancy (V_O) which delivers an excess electronic charge to underlying lattice site Ti^{4+} ions and (ii) interstitial Ti^{3+} ions condensed near the surface by annealing in a vacuum[30-33]. This excess charge allows for dissociative adsorption of O_2 on the 5-fold Ti rows (O_{ad}). Therefore, observation of the valence band spectra can follow up the surface redox reactions. In addition, photon-induced secondary electron emission enabled us to measure work functions which are sensitive to subsurface electronic charge

distributions. As mentioned before, we found out the reaction between O_{ad} atoms and CO molecules which forms CO_2. Scanning tunneling microscope (STM) observations showed that adsorption of an O_2 in a V_O site created a single O_{ad} and direct adsorption of an O_2 on the 5-fold Ti resulted in creation of a paired O_{ad}[30]. Existence of such two types of O_{ad} atoms were confirmed previously by high-resolution medium energy ion scattering (MEIS) using $^{18}O_2$ combined with elastic recoil detection (ERD) of H coming from paired OH, which was created by exposing the surface with V_O vacancies to H_2O molecules[33]. Such surface science techniques provide a powerful tool to investigate the mechanism of emerging catalytic activity of Au nano-clusters in CO oxidation reaction.

All the experiments mentioned above were performed *in situ* under ultrahigh vacuum (UHV) conditions (< 2×10^{-10} Torr) at the beamline 8 named SORIS which was set up at Ritsumeikan SR Center. We deposited Au nano-clusters by molecular beam epitaxy MBE) and determined the average size and shape by MEIS using 120 keV He^+ ions. Photoelectrons as well as secondary electrons excited by synchrotron-radiation-light (20–500 eV) were detected by a concentric hemispherical analyzer with a mean radius of 139.7 mm. In order to measure the amount of the O_{ad} atoms, we employed an isotopically labeled $^{18}O_2$ gas with $^{18}O/^{16}O$ ratio of 95/5. The amount of the ^{18}O atoms adsorbed on the surface was determined by high-resolution MEIS using 80 keV He^+ ions. The details of the SORIS beamline and how to analyze Au nano-clusters by MEIS were described elsewhere[34-36].

We purchased non-doped TiO_2(110) substrates whose surfaces were mirror-finished and chemically etched. The impurities contained in the substrates were less than 5 ppm (less than 0.1 ppm for Mg, Ca, Sr, and Ba). After sputtering with 0.75 keV Ar^+ ions, the as-supplied TiO_2(110) surfaces were annealed at 980 K for 30 min in UHV. Then the substrates became conductive due to creation of Ti interstitials (Ti-int) acting as an electron donor (Ti^{3+}). It must be noted that it is very difficult to prepare a stoichiometric TiO_2(110) surface, because annealing TiO_2(110) surfaces in an O_2 atmosphere causes segregation of Ti-interstitials to the near-surface region leading to formation of added-layers of TiO_2(110) and in many cases resulting in a partially incomplete surface structure such as a Ti_2O_3-like (Ti-rich) clusters[37,38]. Such an incomplete Ti-rich surface is detectable by observing valence band and MEIS spectra. Figures 1 (a) and (b) show typical valence band and MEIS spectra, respectively observed for the Ti-rich surface formed by annealing at 380 K in O_2 ambience of 1×10^{-6} Torr for 10 min. It is clearly seen that the valence band spectrum for the Ti-rich surface is significantly broader than that for the O-rich surface and the MEIS spectrum from O for the Ti-rich surface has a low energy tail and high background level caused by the additional Ti-rich

clusters on the surface. We prepared the *O*-TiO_2(110) surface by dosing an $^{16}O_2$ gas (purity: 99.999 %: 5N) onto reduced surfaces denoted by *R*-TiO_2(110), which were formed by Ar^+ sputtering followed by annealing at 870 K for 10 min in UHV. The above O_2 exposure was carried out starting from a temperature of ~325 K and down to RT at the same O_2 pressure of 1×10^{-6} Torr. Au nano-clusters were then formed on TiO_2(110) surfaces at RT by MBE at a deposition rate of 0.2-0.3 ML/min, where 1 ML is equal to 1.39×10^{15} atoms/cm^2, corresponding to the areal number density of Au(111). We determined the average size and shape (two-dimensional: 2D or three-dimensional: 3D) by high-resolution MEIS[21,35]. Here, 2D-cluster was defined as that with a height below two-atomic layers and the 3D shape was approximated as a partial sphere with a diameter *d* and height *h*.

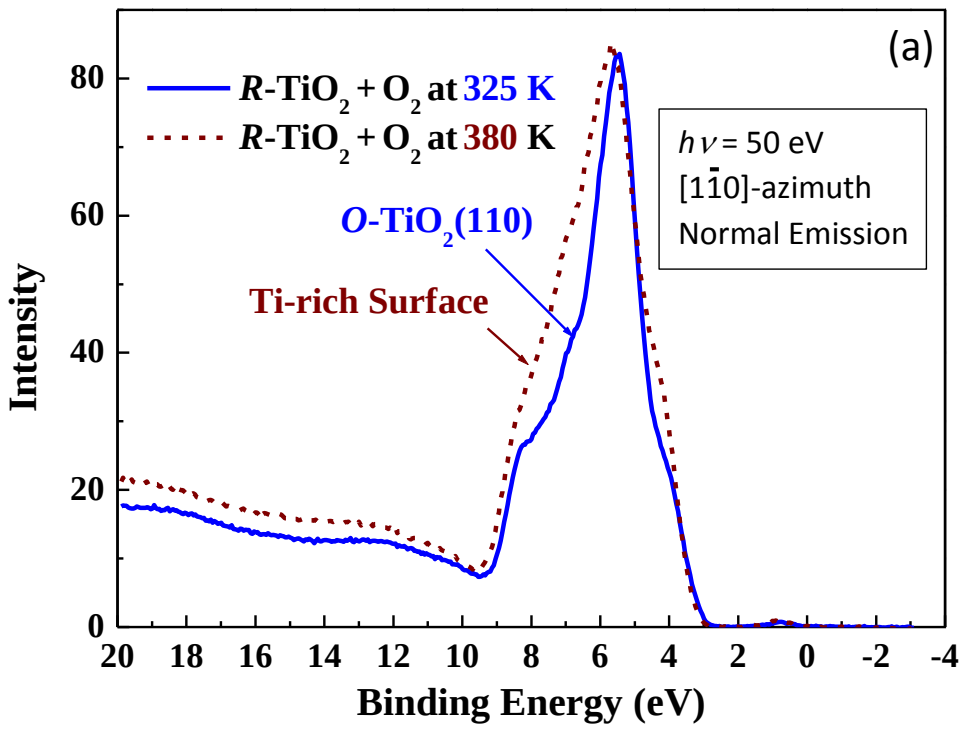

Fig. 1. (a) Valence band spectra taken at incident photon energy of 50 eV for *R*-TiO_2(110) surfaces exposed to O_2 (1×10^{-6} Torr) for 10 min at temperatures from 325 K down to RT (solid curve) and at 380 K (dashed curve).

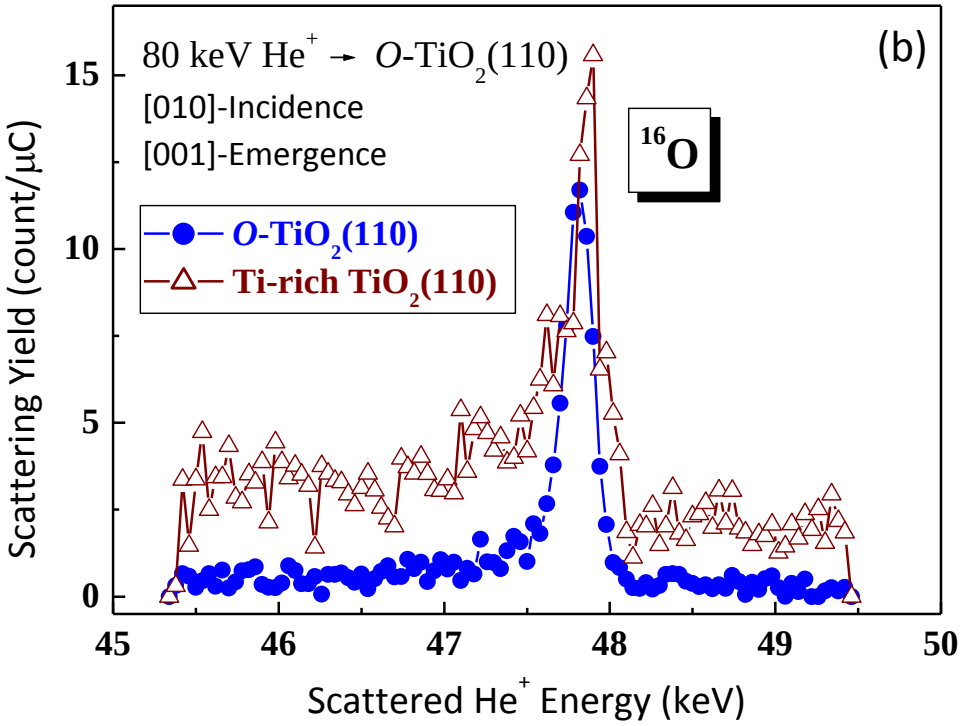

Fig. 2. (b) MEIS spectra observed for 80 keV He^+ ions scattered from O of *R*-TiO_2 oxidized at 325 K - RT (*O*-TiO_2: full circles) and of that oxidized at 380 K (Ti-rich surface: open triangles).

III. CO OXIDATION REACTION

As mentioned before, we found that the O_{ad} atoms adsorbed on the 5-fold Ti reacted with CO molecules to form CO_2 at RT and the Au nano-clusters grown on the O-rich TiO_2(110) surface enhanced the oxidation reaction[21,22]. More exactly, the Au nano-clusters on the *O*-TiO_2(110) surface lowered the barrier for the reaction between O_{ad} and CO resulting in no O_{ad} after CO exposure above 12000 L (1 L = 1×10^{-6} Torr s), while on the O-rich TiO_2(110) surface only about a half of the O_{ad} atoms reacted with CO molecules. This can be confirmed in such a way that both *O*-TiO_2 and Au/*O*-TiO_2 are exposed to CO gas and then further to $^{18}O_2$ gas. The amount of ^{18}O adsorbed on the surface after CO exposure followed by $^{18}O_2$ dose corresponds to that of the O_{ad} atoms which reacted with CO. It was also shown that the number of O_{ad} was increased ~1.5 times for Au/*O*-TiO_2 than that for *O*-TiO_2(110) only[21]. This was demonstrated by detecting ^{18}O for Au/*O*-TiO_2(110) after additional $^{18}O_2$ dose. Of course, in this case the excess electronic charge should still exist in the sub-surface region. Note that the

coverage of the O_{ad} is limited to less than ~10 % (100 %: 5.2×10^{14} atoms/cm^2 corresponds to the areal number density of TiO_2(110)). This is due to the fact that the O_{ad} is a negative species and thus a higher coverage of O_{ad} makes the surface energetically instable just like polar surfaces of alkali halide crystals. Indeed, DFT calculations revealed that the O_2-dissociation barrier is increased from ~0.3 to ~0.8 eV with increasing the number of O_{ad} atoms and thus the maximum coverage (density) is expected to be ~10 % at most[30].

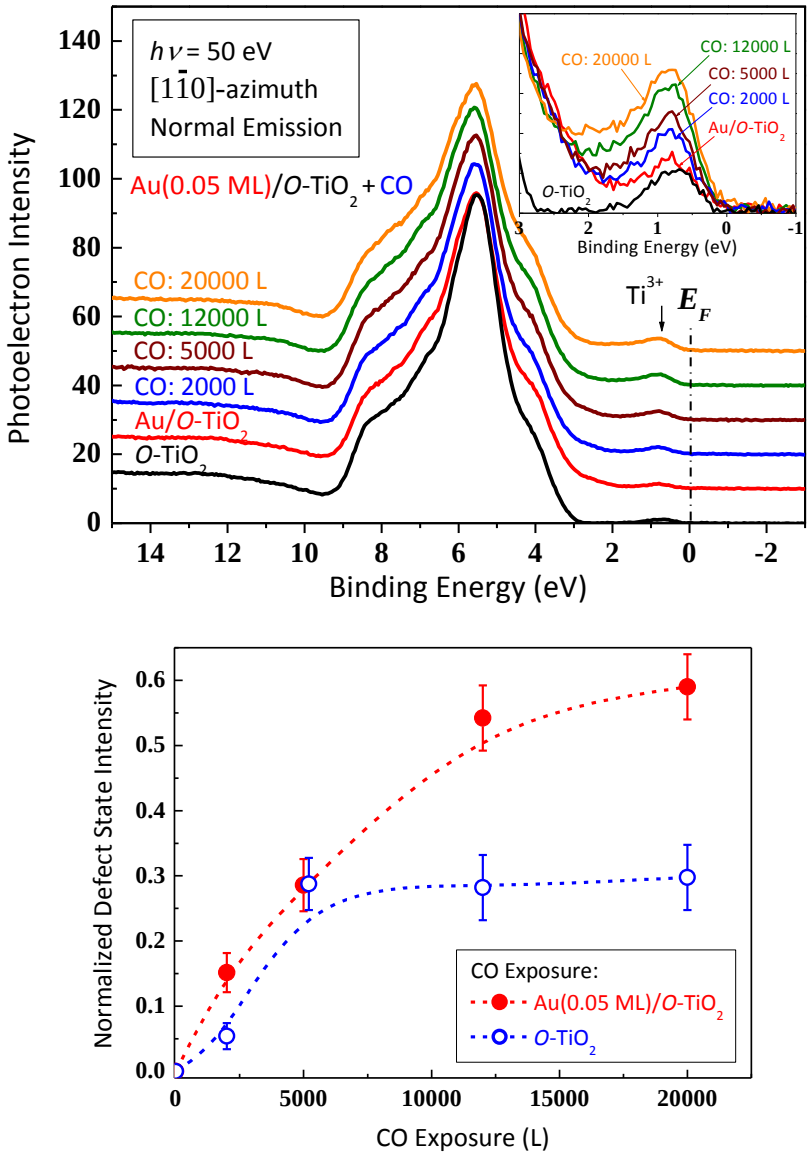

Fig. 2. (Upper) Valence band spectra observed for *O*-TiO_2, Au(0.05 ML)/*O*-TiO_2, and that dosed with CO (2000, 5000, 12000, and 20000 L) at a photon energy of 50 eV under normal emission condition. Inset indicates magnified spectra from the defect (gap) state. (Bottom) Defect state intensity normalized by that for *R*-TiO_2(110) as a function of CO dose for *O*-TiO_2(110) (open circles) and Au(0.05 ML)/*O*-TiO_2(110) (full circles). Sold curves are spline functions drawn to guide the eyes.

This study has confirmed the reproducibility of the above facts and also added some new data. Figure 2(a) shows the valence band spectra observed for *O*-TiO_2, Au(0.05 ML)/*O*-TiO_2, and those exposed to CO (2000, 5000, 12000, and 20000 L). The inset indicates the magnified spectra from the defect state with the binding energy (E_B) of ~0.85 eV below E_F, whose intensity increases with CO dose. Here, Au deposition of 0.05 ML on *O*-TiO_2 resulted in formation of 2D clusters with an average lateral size of ~1.5 nm and two atomic-layer height[21]. The slightly increased background for Au/*O*-TiO_2 comes from Au 6s band. Obviously the defect state intensity (Ti^{3+}) increases with increasing CO dose. The defect (gap) state intensities normalized by that for *R*-TiO_2(110) are depicted as a function of CO dose in Fig. 2(b). The increase in the defect state intensity is attributed to elimination of O_{ad} atoms via oxidation reaction between O_{ad} and CO. The defect state intensity for Au(0.05 ML)/*O*-TiO_2 is almost saturated above 20000 L for CO exposure and almost twice that for *O*-TiO_2 only. Note that the areal occupation ratio of Au nano-clusters was small enough, ~2.5 % at most for Au coverage of 0.05 ML[21]. The above result combined with MEIS and ERD analyses using $^{18}O_2$ and H_2O gases demonstrated that almost all of O_{ad} atoms reacted with CO for Au(0.05 ML)/*O*-TiO_2, whereas nearly a half of O_{ad} atoms still existed for *O*-TiO_2 after CO dose of 20000 L, as reported previously[21,22]. Simultaneously, we measured the work functions for *O*-TiO_2, Au(0.05 ML)/*O*-TiO_2, and those exposed to CO gas (2000, 5000, 12000, and 20000 L), which are shown in Fig. 3(a) and are plotted as a function of CO exposure in Fig. 3(b). After Au deposition of 0.05 ML on *O*-TiO_2 the work function drops from 5.15±0.03 to 4.97±0.03 eV. This indicates an electronic charge transfer from Au to *O*-TiO_2 support, which induced an interface dipole with a polarity of a positive charge on the vacuum side. The interface dipole moment μ_e can be roughly estimated by the relation of $en_d\mu_e/\varepsilon_0 = \Delta\Phi$, where $\Delta\Phi$ = 0.18 eV (reduction of the work function), and e, ε_0, and n_d, respectively are electron charge, permittivity of vacuum, and the number of dipoles per unit area, corresponding to the areal number density of Au clusters ($n_d = 1.4\times10^{16}$ m^{-2} for Au coverage of 0.05 ML). Thus, μ_e is deduced to be ~1×10^{-28} [C m] ≅ 30 [D] (Debye unit). This dipole moment is almost 16 times that of an H_2O molecule. With increasing CO dose the work functions for both *O*-TiO_2 and Au/*O*-TiO_2 are decreased owing to elimination of O_{ad} by the reaction of O_{ad} with CO, because the O_{ad} atom is an electronegative species and thus withdraws a subsurface excess electronic charge. The existence of the O_{ad} atoms induces a surface dipole, as depicted in Fig. 4 and thus results in an upward band bending, a lower E_B shift, and a larger work function. Therefore, elimination of the O_{ad} leads to decrease in work function. The reduction of the

work function is 0.40±0.3 eV for *O*-TiO_2 after CO exposure of 20000 L, which is slightly larger than that for Au/*O*-TiO_2 despite the fact that almost a half of O_{ad} still exist on the *O*-TiO_2 after a CO dose of 20000 L, while almost all of O_{ad} reacted with CO on Au/*O*-TiO_2. This indicates that with decrease in O_{ad} coverage the transferred electrons from Au to *O*-TiO_2 support return back slightly, contributing to increase in the work function. This is confirmed later by the work functions measured for Au(0.05 ML)/*O*-TiO_2 before and after O_2 exposure.

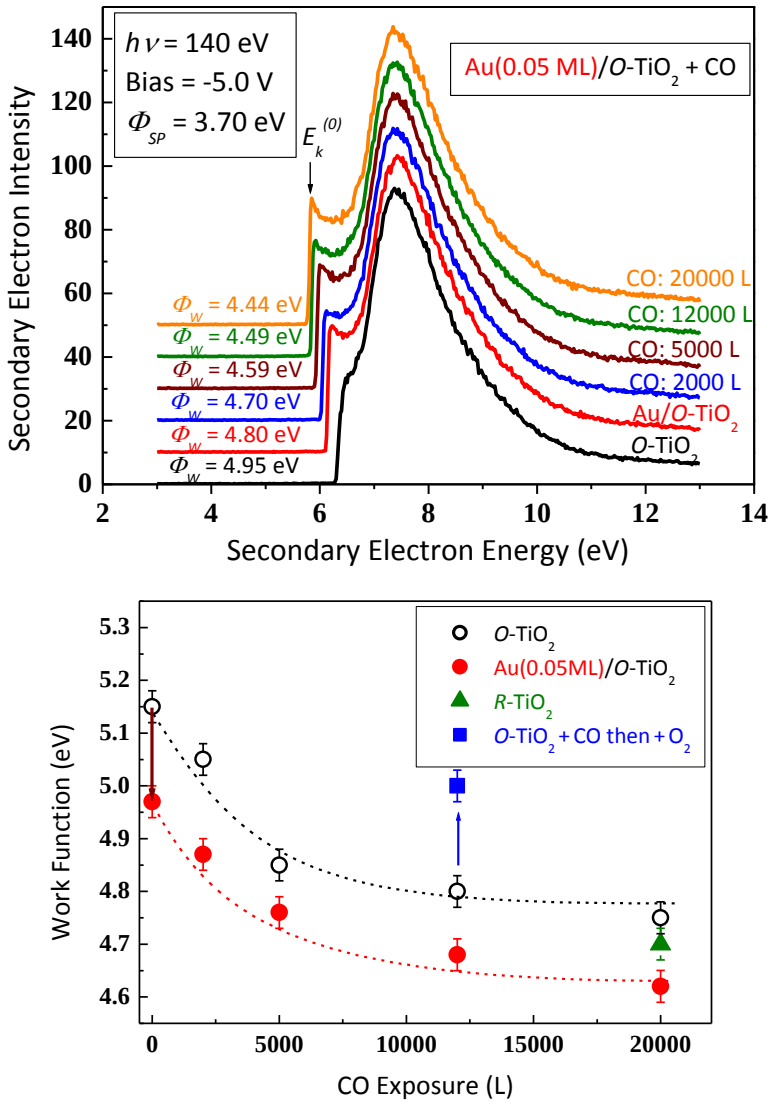

Fig. 3. (Upper) Secondary electron emission spectra observed for 140 eV photon incidence on *O*-TiO_2, Au(0.05 ML)/*O*-TiO_2, and that exposed to CO with dose of 2000, 5000, 12000, and 20000 L from bottom to top. (Bottom) Work functions observed for *R*-TiO_2 (triangle), *O*-TiO_2 (open circles), Au(0.05 ML)/*O*-TiO_2 (full circles) before and after CO exposure. Square symbol denotes work function measured for *O*-TiO_2 after CO exposure of 12000 L and then dosed with O_2 (2000 L).

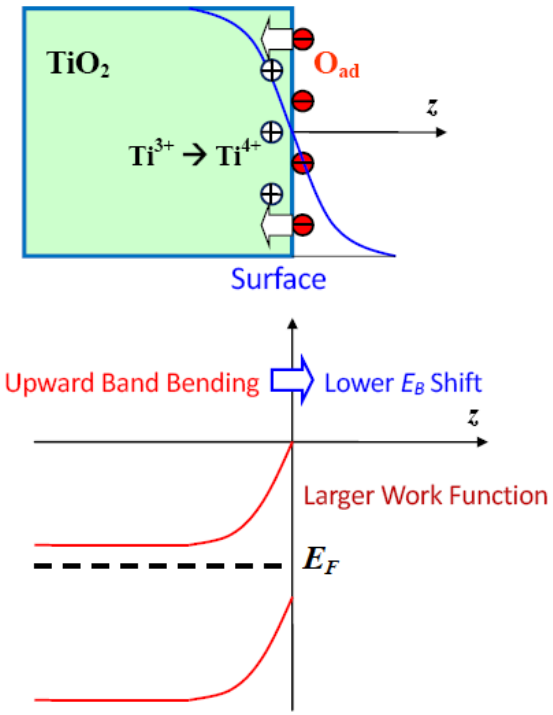

Fig. 4. Schematic of surface dipole of O_{ad} withdrawing subsurface electronic charge and leading to upward band bending.

In the above observations, the number of O_{ad} atoms on the *O*-TiO_2(110) surface was unchanged after Au deposition of 0.05 ML (areal occupation: ~2.5 %). Therefore, it is clear that presence of Au nano-clusters on *O*-TiO_2 lowers the barrier for the reaction between O_{ad} and CO. In addition, the Au/*O*-TiO_2 system increases the number of O_{ad} adatoms. Figure 5(a) shows the valence band spectra observed for the *O*-TiO_2(110) before and after Au deposition of 0.05 ML on the *O*-TiO_2 surface and for the Au/*O*-TiO_2 after exposure to $^{18}O_2$ gas (1000 L). It is clearly seen that the gap state intensity does not change after Au deposition but after exposure to $^{18}O_2$ the gap state disappears almost completely. This reveals that O_{ad} atoms were further adsorbed on the surface until the subsurface excess electronic charge was consumed completely and the coverage approaches the limited value of ~10 %. Note that the amount of the excess charge (gap state) can be controlled by the number of repetition of the sputtering/annealing cycle. The further adsorption of O_{ad} was also confirmed directly by detecting ^{18}O in the MEIS measurement. Figure 5(b) shows the MEIS spectrum observed for 80 keV He^+ ions scattered from ^{16}O and ^{18}O of the Au/*O*-TiO_2 exposed to $^{18}O_2$ (1000 L). The inset is the magnified spectrum from ^{18}O, indicating the additional O_{ad} of $1.6\pm0.3\times10^{13}$ atoms/cm^2, corresponding to an additional coverage of 3.1 %. We also measured the work functions

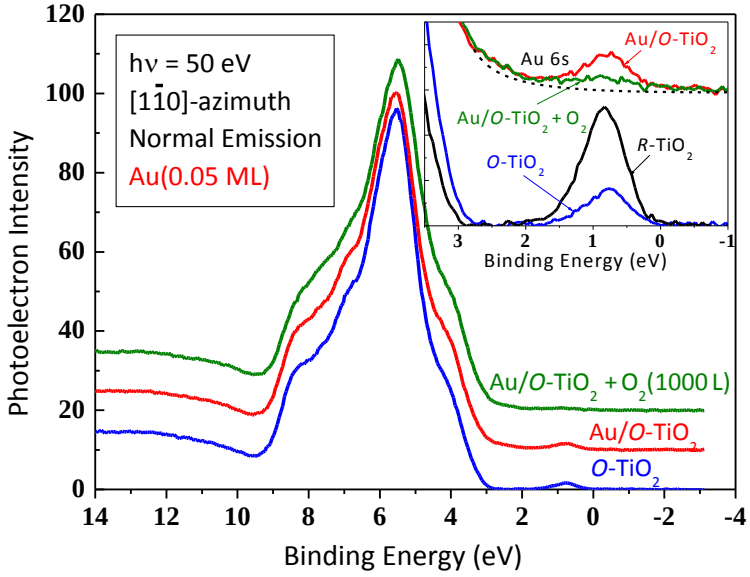

Fig. 5 (a) Valence band spectra observed at photon energy of 50 eV for *O*-TiO_2(110), Au(0.05 ML)/*O*-TiO_2(110), and that after $^{18}O_2$ exposure of 1000 L. Inset shows magnified spectra from gap (defect) state.

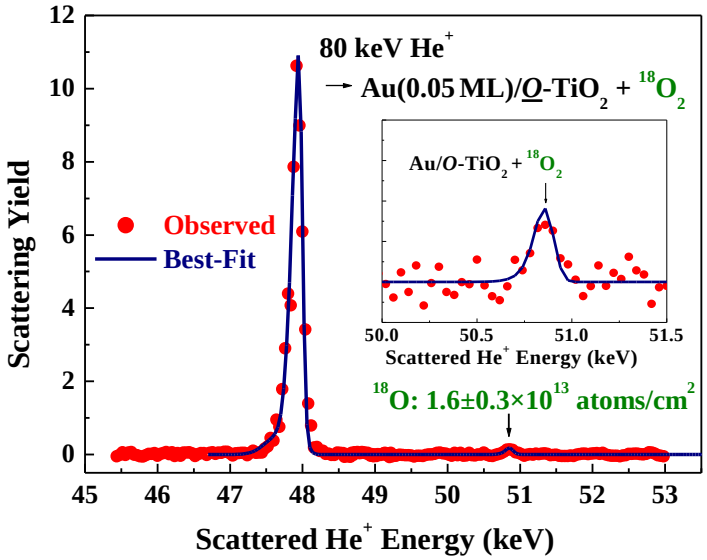

(b) MEIS spectrum observed for 80 keV He^+ ions incident on Au(0.05 ML)/*O*-TiO_2(110) and scattered by ^{16}O and ^{18}O after $^{18}O_2$ exposure of 1000 L. Inset indicates magnified spectrum from ^{18}O.

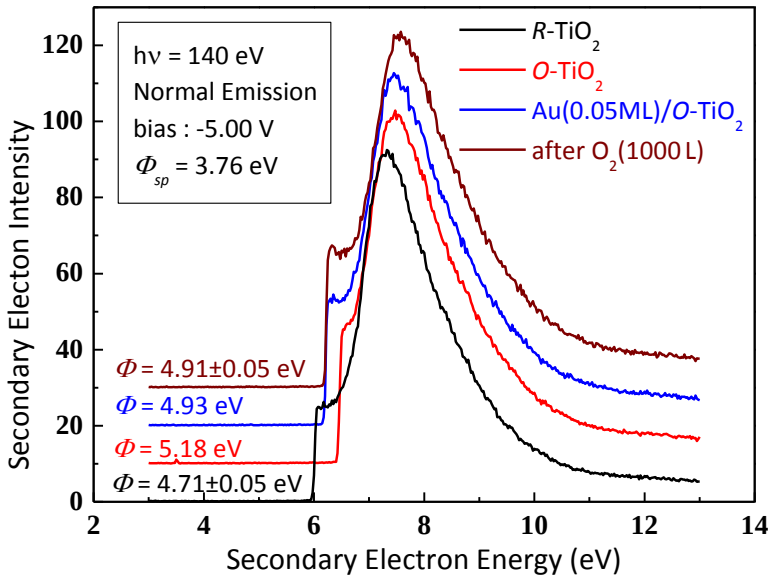

(c) Secondary electron spectra emitted at photon incidence of 140 eV for *R*-TiO_2, *O*-TiO_2, Au(0.05 ML)/*O*-TiO_2 before and after $^{18}O_2$ exposure of 1000 L.

for *R*-TiO_2(110), *O*-TiO_2(110) and Au(0.05 ML)/*O*-TiO_2(110), and that exposed to $^{18}O_2$ (1000 L), as indicated in Fig. 5(c). After $^{16}O_2$ exposure onto *R*-TiO_2, the work function was increased about 0.4 eV due to adsorption of electronegative species of O_{ad} and O_{br} (O_{ad} : filled V_O = 3.5 : 2.5)[33]. Here, if we simply assume that O_{br} and O_{ad} form a same surface dipole, the dipole moment μ_e^O is roughly estimated to be 5.9×10^{-30} [C m] comparable with that of a H_2O molecule (the amount of ^{18}O adsorbed on *R*-TiO_2(110) is ~6×10^{13} atoms/cm^2). Deposition of Au on the *O*-TiO_2 induced the electronic charge transfer from Au to *O*-TiO_2 support and thus the work function was decreased. Interestingly, the work function did not change within experimental uncertainty after exposing Au/*O*-TiO_2 to $^{18}O_2$ gas. The adsorption of O on the surface (O_{ad} and filled V_O) should increase the work function, while the further O adsorption promotes the electronic charge transfer from Au to *O*-TiO_2 support and thus compensates the increase in the work function, as discussed previously. The increase in O_{ad} atoms on Au/*O*-TiO_2 was directly confirmed by MEIS analysis. Figure 6 shows the MEIS spectra observed for *O*-TiO_2(110) and Au(0.05 ML)/*O*-TiO_2(110) which were exposed to CO (300000 L) and then dosed with $^{18}O_2$ (3000 L). The amount of ^{18}O ($^{18}O_{ad}$) detected for Au(0.05 ML)/*O*-TiO_2(110) is $6.3\pm0.5\times10^{13}$ atoms/cm^2 (~12 %), almost twice that (3.6×10^{13} atoms/cm^2: ~7 %) for *O*-TiO_2(110) only. Note that the TiO_2(110) substrate used here underwent many sputtering/annealing cycles and thus accumulated much more excess charge mainly as Ti-interstitials than that described before.

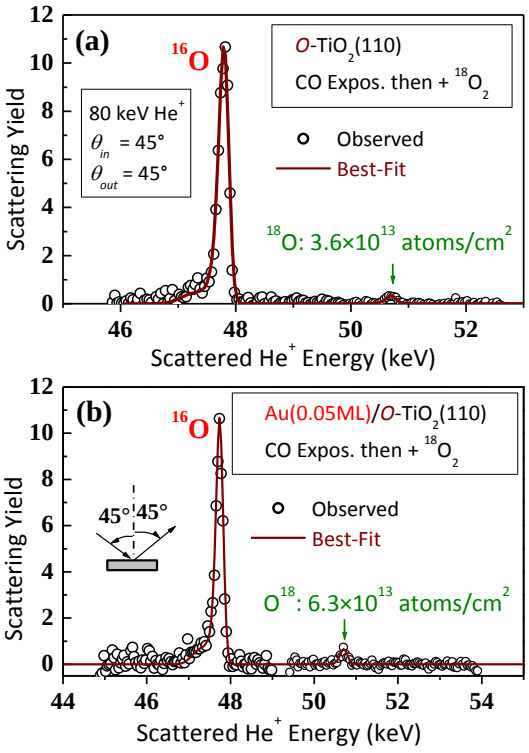

Fig. 6. MEIS spectra observed for 80 keV He^+ ions incident on *O*-TiO_2(110) (upper) and Au(0.05 ML)/*O*-TiO_2(110) (lower) and scattered from ^{16}O and ^{18}O after CO exposure of 300000 L followed by $^{18}O_2$ does of 3000 L.

IV. THE ROLE OF Au NANO-CLUSTERS

Based on the results mentioned above, we consider the role of Au nano-clusters supported on *O*-TiO_2(110) in CO oxidation reaction. Importantly, the interface dipole created by the electronic charge transfer from Au to *O*-TiO_2 support has a polarity of a positive charge on the vacuum side, while the electronegative species of O_{ad} atoms withdraw electrons from underlying subsurface Ti^{3+} ions resulting in formation of a surface dipole with a reverse polarity. The interaction between the two dipoles with anti-parallel polarity is attractive and thus the Au/*O*-TiO_2 interface dipole lowers the potential barrier for O adsorption and stabilizes the O_{ad} adatoms on the 5-fold Ti rows. Despite that, the amount of O_{ad} is saturated at 10 - 12 % because of consumption of the excess electronic charge and of the increase in the potential barrier with increasing the O_{ad} coverage. Actually, too high coverage of the electronegative O_{ad} makes the surface energetically unstable, just like a polar surface of ionic crystals. It was evidenced by Fourier-transform infrared spectroscopy (FTIR) that a CO molecule is adsorbed with the C atom at the head on an Au cluster surface[39]. This seems quite reasonable, because the polar molecule CO has a small dipole moment of 4.1×10^{-31} [C m] with a polarity of −C·O+[40] and the adsorption is enhanced by the attractive interaction between the polar molecule CO and the cationic Au cluster. The adsorbed CO molecule moves promptly to the perimeter interface and reacts with an O_{ad} loosely bound to 5-fold Ti rows to form CO_2. Note here that CO molecules are not adsorbed on TiO_2(110) at RT except for at low enough temperatures[41]. This scenario is quite the same as that of the second reaction path predicted by Wang and Hammer[15]. Figure 7 illustrates the schematic of the *interface dipole model* which explains the mechanism of CO oxidation reaction with O_{ad} over Au/*O*-TiO_2(110) model catalyst. According to the DFT calculations by Wang and Hammer[15], an O_2 molecule is bound at the Au/*O*-TiO_2 interface and a CO binds to 2nd-layer Au site and then one O atom reacts with the CO and the other O is left at the interface. This is the first reaction path. The *cationic cluster model* is consistent with our experimental data, except for the following point. This model claims that binding the O_2 to the Au/O-TiO_2 interface further depletes the Au-5d states by $0.22e^-$. However, our experiment showed that the gap state completely disappeared after O_2 exposure for Au/*O*-TiO_2. This indicates that the excess electronic charge of Ti^{3+} is consumed to bind the O_2 or O_{ad} at the Au/*O*-TiO_2 interface.

Finally, we discuss the *d-band model* proposed by Hammer and Nørskov[12-14] to explain the general trends in heterogeneous catalysis, which advocates a scenario that as the d-band center position (E_d) for a transition metal moves toward the Fermi level, the potential barrier becomes lower for the dissociative adsorption of molecules on the metal

surface. It is predicted that with decreasing the coordination number of the metal, in particular, with decreasing the metal cluster size the E_d value shifts toward the Fermi level. We previously determined the d-band center position (E_d) for Au nano-clusters on amorphous carbon films as a function of the size from ~10 up to ~1500 atoms/cluster[24]. The result obtained shows that the E_d value moves apart from the Fermi level with decreasing the size below ~150 atoms/cluster (diameter: ~2.5 nm), although the E_d values were still closer to the Fermi level than that for the bulk value (see Fig. 8). The d-band width (W_d) is well correlated with the d-band center and decreased rapidly below the critical size (~150 atoms/cluster), as shown in Fig. 8.

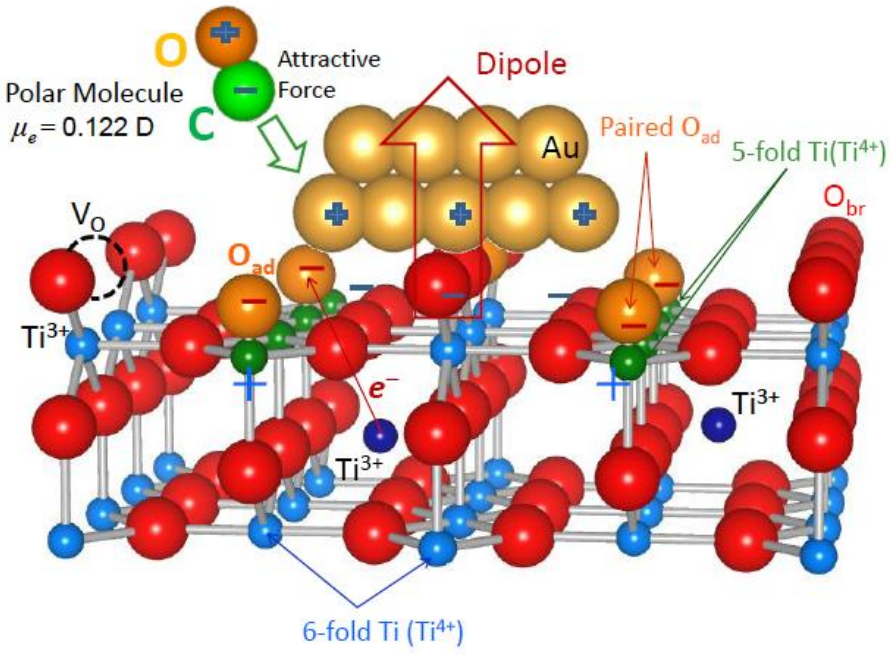

Fig. 7. Schematic of probable mechanism of emerging catalytic activity of Au/*O*-TiO_2(110) model catalyst in CO oxidation reaction.

The cluster-size dependent Pt-Pt and Au-Au bond lengths measured by transmission electron microscope[42] and extended X-ray absorption fine structure[43,44] showed considerable contractions for the cluster size below ~2.5 nm, which coincides well with the above critical size. The observed maximum contraction was ~10 % for Pt-clusters at a size of $d \cong 1.5$ nm and ~6 % for Au-clusters at $d \cong 1$ nm. Xu and Mavrikakis[45] calculated the barrier for O_2 dissociation on tensile-strained Au(111) and Au(211) surfaces and found notable decreases in the barrier height, indicating significant changes in the surface band structure.

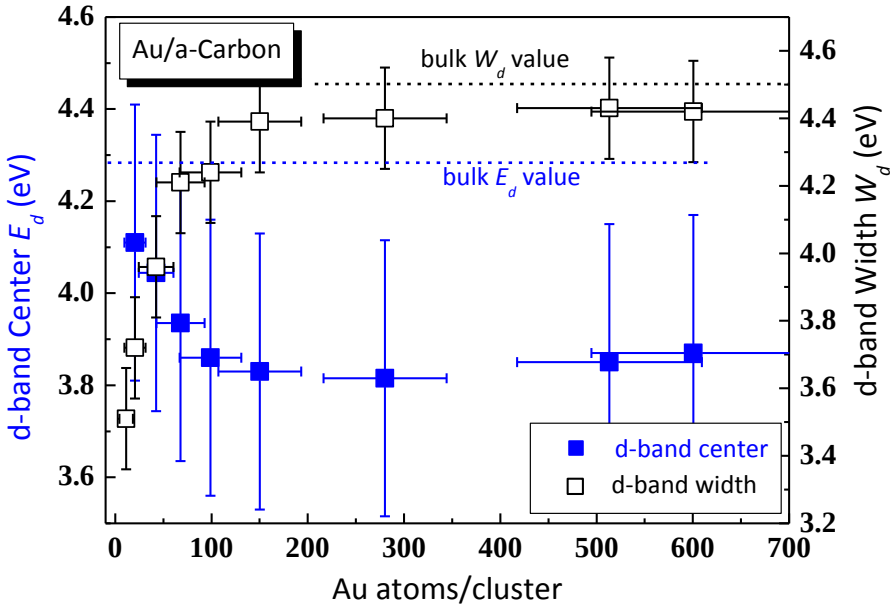

Fig. 8. d-band center position E_d scaled from Fermi level (full squares) and d-band width W_d (open squares) determined experimentally for Au nano-clusters on amorphous carbon film, as a function of cluster size (atoms/cluster). Dashed lines indicate bulk values.

We have investigated the tensile strain effect upon the d-band center position using the Vienna *ab initio* simulation package (VASP)[26,27]. The periodic unit cell was set to 2.8×2.8×2.8 nm^3 to keep a sufficient separation between Au clusters. We adopted the local density approximation (LDA) as the exchange-correlation potential, which gave rise to better equilibrium Au-Au inter-atomic distances in bulk test calculations than the generalized gradient approximation (GGA). The relaxation procedure was continued until the force acting on each atom was smaller than 0.01 eV/Å. The cut-off energy for the plane wave basis set was set to 300 eV. We calculated the average Au-Au bond length and d-band center position for Au_{19}, Au_{38}, and Au_{55} clusters with O_h symmetry. Figure 9 shows the d-band center position and the Au-Au bond length for the Au_{19}, Au_{38}, and Au_{55} clusters with relaxed and fixed bulk bond length, which correspond to coordination numbers of 6.32, 7.58, and 7.86, respectively estimated from the formula reported by Hardeveld and Harog[46]. The Au-Au bond lengths calculated here (2.767, 2.801, 2.803 Å) are consistent with those (2.75, 2.78, 2.79 Å) given by Häberlen et al.[44]. It is found that the d-band center position for the relaxed Au clusters moves apart from the Fermi level compared with that for the fixed bond length, although significant correlation is not seen between the d-band center and average coordination number, probably due to quite different ratio of corner, edge and surface atoms for each size model. We calculated the d-band center for Au_{38} cluster keeping the O_h symmetry in a

free state as a function of Au-Au bond length, as shown in Fig. 10. It is clearly seen that the d-band center shifts apart from the Fermi level with increasing the tensile strain. This trend is also seen for Au_{55} clusters. The contraction of the Au-Au bond length probably takes place on amorphous carbon and TiO_2 supports because of weak interactions between Au and the supports, although the Au clusters takes partial sphere shape on amorphous carbon[24] and 2D-cluster shape with two atomic-layer height on the TiO_2(110) support for Au coverage below 0.2 ML. It is generally expected quantum mechanically that the band gap is increased with decreasing the bond length. Indeed, Valden et al.[5] reported that a metal-to-nonmetal transition occurs as the Au cluster size is decreased below 3.5 nm in diameter and 1.0 nm in height. The result obtained here provides a deeper insight into the shift of the d-band center position apart from the Fermi level for Au nano-clusters with the size below ~2.5 nm (critical size). This is in contradiction with the previous report of Phala and van Steen[25] who did not consider the strain effect. The present result clearly explains our previous experimental observation that the d-band center moves apart from the Fermi level with decreasing the cluster size below ~2.5 nm. Such a lattice contraction is a general trend for metal nano-clusters due to the surface tension[47]. Therefore, it is concluded that the *d-band model* cannot fully explain the catalytic activities of metal nano-clusters for dissociative adsorption of molecules on the metal cluster surfaces.

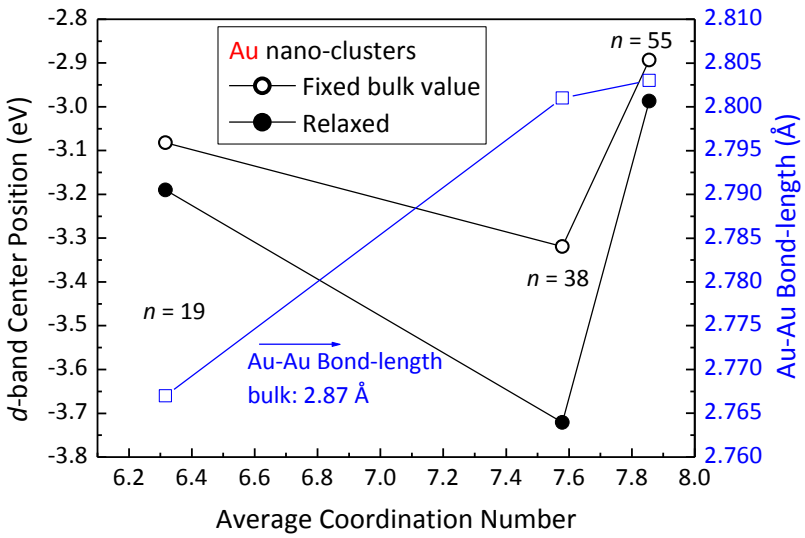

Fig. 9. d-band center position E_d and Au-Au bond length calculated using VASP for Au_{19}, Au_{38}, and Au_{55} with O_h symmetry. The abscissa indicates the corresponding coordination number estimated from the literature[46].

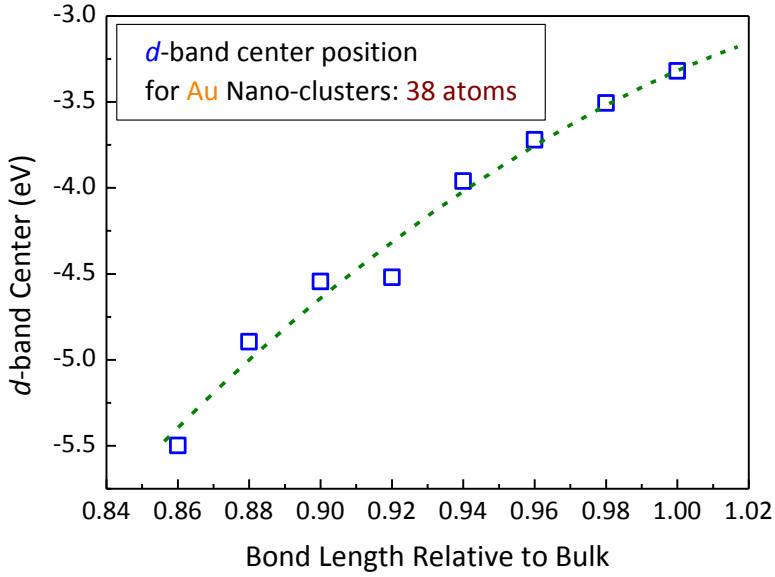

Fig. 10. d-band center position E_d calculated by VASP for Au_{38} clusters keeping O_h symmetry, as a function of Au-Au bond length normalized by the bulk value.

V. CONCLUSION

We have checked the reproducibility of the previous results and performed additional observations for CO oxidation reaction over Au nano-clusters supported on rutile TiO_2(110). The results obtained have evidenced again that the O_{ad} atoms adsorbed on the 5-fold Ti react with CO to form CO_2 and the electronic charge transfer takes place from Au nano-clusters to O-rich rutile TiO_2(110) substrates, which plays a crucial role to enhance the catalytic activity. The interface dipole formed by the above electronic charge transfer has a polarity of a positive charge on the vacuum side, which allows for promoting O adsorption on the 5-fold Ti rows, because the electro-negative species of O_{ad} withdraws an electronic excess charge from subsurface Ti^{3+} ions (gap state), resulting in formation of a dipole with a reverse polarity. Such a situation leads to increase in number of O_{ad} atoms and thus to complete disappearance of the gap state. High-resolution MEIS has evidenced directly the additional $^{18}O_{ad}$ atoms for Au/*O*-TiO_2(110) dosed with $^{18}O_2$ gas. It is also revealed that almost all of O_{ad} atoms react with CO for Au/*O*-TiO_2(110), whereas the reacted ones are about half of O_{ad} for *O*-TiO_2(110) only. This is ascribed to the attractive interaction between the cationic Au clusters and a polar molecule of −CO+. The polarized CO molecules are thus incident on

the *O*-TiO_2 surface with the C-O bond perpendicular to the surface and with the C atoms at the head. Such a behavior was demonstrated by infrared spectroscopy. The CO oxidation takes place via reaction of the adsorbed CO with the O_{ad} at the Au/*O*-TiO_2 perimeter interface. The CO oxidation occurred most effectively for Au coverage of 0.05 ML. In this case, the Au clusters take a 2D-shape with two atomic layer height and average lateral size of ~1.5 nm (areal occupation: ~2.5 %). It is not clear at the present whether the *interface dipole model* proposed here for the Au/*O*-TiO_2(110) model catalyst can be applied or not to Au/supports real catalysts, because additional factors such as OH and some environmental inclusions may play an important role in the real catalysts[18,48].

We have also considered the other models based on the DFT calculations. The *cationic cluster model* proposed by Wang and Hammer explains well our experimental data except for the following point that binding an O_2 molecule to the Au/O-TiO_2 interface further depletes the Au-5d states by $0.22e^-$. Our experiment, however, has showed that the gap state completely disappeared after O_2 exposure for Au/*O*-TiO_2, indicating that the excess electronic charge of Ti^{3+} is consumed to bind the O_2 or O_{ad} at the Au/*O*-TiO_2 interface. The *d-band model* widely accepted to explain the emerging activities of heterogeneous catalysts claims that with decreasing metal-cluster size the d-band center position shifts toward the Fermi level and thus lowers the potential barriers for dissociative adsorption of molecules on the surface. Our previous study[24], however, revealed that the d-band center position for gold nano-clusters on amorphous carbon moved apart from the Fermi level with decreasing the cluster size. Based on the *ab initio* calculations (VASP), it is demonstrated that this was attributed to contraction of the Au-Au bond length with decreasing the cluster size. Such a contraction of bond-length is a general trend in metal nano-clusters. Therefore, the *d-band model* cannot be invoked to explain the enhanced catalytic activities of Au nano-clusters in such a CO oxidation reaction.

Finally, it is pointed out again that the subsurface electronic excess charge plays a crucial role in surface electrochemistry such a gas phase reaction over the TiO_2(110) and Au/TiO_2(110). The gap state as an electronic excess charge is created by sputtering/annealing cycles for rutile-TiO_2(110) surfaces and can be detected by photoelectron spectroscopy. The dynamics of the CO oxidation reaction can be also followed by ion scattering coupled with elastic recoil detection analysis using the isotopically labeled $^{18}O_2$ and $^{2}D_2O$ gases. Therefore, approaches based on physics are welcomed and inspired to investigate catalytic activities, which have been opened only to chemistry.

ACKNOWLEDGMENTS

This work was partly supported by Japan Science and Technology Agency, JST, CREST.

References

[1] M. Haruta, T. Kobayashi, H. Sano, and N. Yamada, Chem. Lett. **2**, 475 (1987).

[2] S.D. Lin, M. Bollinger, and M.A. Vannice, Catal. Lett. **17**, 245 (1993).

[3] Y. Yuan, K. Asakura, H. Wan, K. Tsai, and Y. Iwasawa, Catal. Lett. **42**, 15 (1996).

[4] M. Haruta, Catal. Today **36**, 153 (1997).

[5] M. Valden X. Lai, and D.W. Goodman, Science **281**, 1647 (1998).

[6] M.M. Shubert, S. Hackenberg, A.C. van Veen, M. Muhler, V. Pluzak, and R.J. Behm, J. Catal. **197**, 113 (2001).

[7] N. Lopez, T.V.W. Janssens, B.S. Clausen, Y. Xu, M. Mavrikakis, T. Bligaard, and J.K. Nørskov, J. Catal. **223**, 232 (2004).

[8] Z. Yan, S. Chinta, A.A. Mohamed, J.P. Fackler, and D.W. Goodman, Catal. Lett. **111**, 15 (2006).

[9] T.V.W. Janssens, B.S. Clausen, B. Hvolbæk, H. Falsig, C.H. Christensen, T. Bligaard, and J.K. Nørskov, Top. Catal. **44**, 15 (2007).

[10] B. Hvolbæk, T.V.W. Janssens, B.S. Clausen, H. Falsig, C.H. Christensen, and J.K. Nørskov, Nanotoday **2**, 14 (2007).

[11] Y. Zhou, N.J. Lawrence, L. Wang, L. Kong, T-S. Wu, J. Liu, Y. Gao, J.R. Brewer, V.K. Lawrence, R.F. Sabirianov, Y-L. Soo, X.C. Zeng, P.A. Dowben, W.N. Mei, and C.L. Cheung, Angew. Chem. Int. Ed. **52**, 6936 (2013).

[12] B. Hammer and J.K. Nørskov, Nature **376**, 238 (1995).

[13] B. Hammer and J.K. Nørskov, Adv. Catal. **45**, 71 (2000).

[14] T. Bligaard and J.K. Nørskov, Electrochem. Acta **52**, 5512 (2007).

[15] J.G. Wang and B. Hammer, Phys. Rev. Lett. **97**, 136107 (2006).

[16] D. Matthey, J.G. Wang, S. Wendt, J. Matthiesen, R. Schaub, E. Lægsgaard, B. Hammer, and F. Besenbacher, Science **315**, 1692 (2007).

[17] M. Kotobuki, R. Leppelt, D.A. Hansgen, D. Widmann and R.J. Behm, J. Catal. **264**, 67 (2009).

[18] T. Fujitani and I. Nakamura, Angew. Chem. **50**, 10144 (2011).

[19] I.X. Green, W. Tang, M. Neurock, and J.T. Yates, Jr., Science **333**, 736 (2011).

[20] D. Widmann and R.J. Behm, Angew. Chem. Int. Ed. **50**, 10241 (2011).

[21] K. Mitsuhara, M. Tagami, T. Matsuda, A. Visikovskiy, M. Takizawa, and Y. Kido, J. Chem. Phys. **136**, 124303 (2012).
[22] K. Mitsuhara, H. Okumura, A. Visikovskiy, M. Takizawa, and Y. Kido, Chem. Phys. Lett. **513**, 84 (2011).
[23] H. Shi, M. Kohyama, S. Tanaka, and S. Takeda, Phys. Rev. **B 80**, 155413 (2009).
[24] A. Visikovskiy, H. Matsumoto, K. Mitsuhara, T. Nakada, T. Akita, and Y. Kido, Phys. Rev. **B 83**, 165428 (2011).
[25] N.S. Phala and E. van Steen, Gold Bulletin **40**, 150 (2007).
[26] G. Kresse and J. Hafner, Phys. Rev. **B 47**, 558 (1993).
[27] G. Kresse and J. Furthmüller, Phys. Rev. **B 54**, 11169 (1996).
[28] R.L. Kurtz, R. Stockbauer, T.E. Madey, E. Román, and J.L. de Segovia, Surf. Sci. **218**, 178 (1989).
[29] Z. Zhang, S-P. Jeng, and V.E. Henrich, Phys. Rev. **B 43**, 12004 (1991).
[30] S. Wendt, P.T. Sprunger, E. Lim, G.K. Madsen, Z. Li, J.Ø. Hansen, J. Matthyiesen, A. Blekinge-Rasmussen, E. Lægsgaard, B. Hammer, and F. Besenbacher, Science **320**, 1755 (2008).
[31] C.M. Yim, C.L. Pang, and G. Thornton, Phys. Rev. Lett. **104**, 036806 (2010).
[32] Z. Dohnálek, I. Lyubinetsky, and R. Rousseau, Prog. Surf. Sci. **85**, 161 (2010).
[33] K. Mitsuhara, H. Okumura, A. Visikovskiy, M. Takizawa, and Y. Kido, J. Chem. Phys. **136**, 124707 (2012).
[34] Y. Kido, H. Namba, T. Nishimura, A. Ikeda, Y. Yan and A. Yagishita, Nucl. Instrum. Methods **B 136-138**, 798 (1998).
[35] H. Matsumoto, K. Mitsuhara, A. Visikovskiy, T. Akita, N. Toshima and Y. Kido, Nucl. Instrum. Methods **B 268**, 2281 (2010).
[36] K. Mitsuhara, H. Okumura, T. Matsuda, M. Tagami, A. Visikovskiy and Y. Kido, Nucl. Instrum. Methods **B 276**, 56 (2012).
[37] L.P. Zhang, M. Li, and U. Diebold, Surf. Sci. **412/413**, 242 (1998).
[38] U. Diebold, Surf. Sci. Rep. **48**, 53 (2003).
[39] F. Boccuzzi, A. Chiorino, M. Manzoli, P. Lu, T. Akita, S. Ichikawa, and M. Haruta, J. Catal. **202**, 256 (2001).
[40] J.S. Muenter, J. Mol. Spectroscopy **55**, 490 (1975).
[41] Z. Wang, Y. Zhao, X. Cui, S. Tan, A. Zhao, B. Wang, J. Yang, and J.G. Hou, J. Phys. Chem. **C 114**, 18222 (2010).
[42] M. Klimenkov, S. Nepijko, H. Kuhlenbeck, M. Bäumer, R. Schlögl, and H.-J Freund, Surf. Sci. **391**, 27 (1997).
[43] J.T. Miller, A.J. Kropf, Y. Zha, J.R. Regalbuto, L. Delannoy, C. Louis, E. Bus, and

J.A. van Bokhoven. J. Catal. **240**, 222 (2006).
[44] O.D. Häberlen, S. Cheong, M. Stener, and N. Rösch, J. Chem. Phys. **106**, 5189 (1997).
[45] Y. Xu and M. Mavrikakis, J. Phys. Chem. **B 107**, 9298 (2003).
[46] R.V. Hardeveld and F. Harog, Surf. Sci. **15**, 189 (1969).
[47] Z. Huang, P. Thomson, and S. Di, J. Phys. Chem. Solids **68**, 530 (2007).
[48] A. Bongiorno and U. Landman, Phys. Rev. Lett. **95**, 106102 (2005).